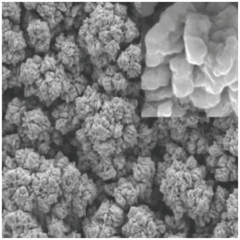

Interfacing metals and compounds for enhanced hydrogen evolution from water splitting

Jian-Hong Tang and Yujie Sun

Hydrogen production from water electrolysis with renewable energy input has been the focus of tremendous attention, as hydrogen is widely advocated as a clean energy carrier. In order to realize large-scale hydrogen generation from water splitting, it is essential to develop competent and robust electrocatalysts that will substantially decrease the overpotential requirement and improve energy efficiency. Recent advances in electrocatalyst design reveal that interfacial engineering is an effective approach in tuning the adsorption–desorption abilities of key catalytic intermediates on active sites, accelerating electron transfer, and stabilizing the active sites for long-term operation. Consequently, a large number of hybrid electrocatalysts consisting of metal/compound interfaces have been demonstrated to exhibit superior performance for electrocatalytic hydrogen evolution from water. This article highlights examples of these hybrid electrocatalysts, including noble metal and non-noble metal candidates interfaced with a variety of compounds. Specific emphasis is placed on the synthetic methods, reaction mechanisms, and electrocatalytic activities, which are envisioned to inspire the design and development of further improved electrocatalysts for hydrogen evolution from water splitting on an industrial scale.

Introduction

With the rapid growth of global energy demands and increasing environmental concerns, intense research efforts have been devoted to exploring sustainable and "green" energy sources as viable alternatives to fossil fuels.[1–6] Among these approaches, renewable energy-driven H_2 evolution from electrocatalytic water splitting is considered a promising pathway because of the zero carbon release nature of this process as well as the high gravimetric energy density of H_2.[7–15] The H_2 evolution reaction (HER) is the reductive half-reaction of water electrolysis, which is generally carried out under either strong acidic or alkaline conditions for better electrolyte conductivity.[16,17] HER at low pH ($2H^+ + 2e^- \leftrightarrow H_2$) typically exhibits high energy efficiency and requires a compact design with proton exchange membranes. Nevertheless, the limited scope of suitable low-cost electrocatalysts under strongly acidic conditions and potential degradation of the membrane restrict its wide application. On the other hand, H_2 production in alkaline electrolytes ($2H_2O + 2e^- \leftrightarrow H_2 + 2OH^-$) shows unique advantages, such as a wider library of suitable earth-abundant electrocatalysts. Nevertheless, the overall performance of HER under alkaline condition is largely limited by the sluggish kinetics of water adsorption and dissociation, leading to low efficiency, high overpotential, and large energy consumption.[16] To date, significant efforts have been made to develop competent low-cost electrocatalysts for HER with high activity and long durability. A large number of catalyst candidates, including metals, alloys, and metal compounds, have been explored for effective H_2 production from water electrolysis.

Among many design approaches in achieving competent HER electrocatalysts, interface engineering has emerged as an effective strategy, which can optimize the adsorption/desorption of catalytic intermediates, accelerate electron transfer, and stabilize active sites.[16,18–20] Various combinations of metals (Pt, Au, Ru, Rh, Pd, Ni, Co, Fe, Cu), alloys (Ni-Co, Ni-Mn, Ni-Mo), and compounds (oxides, hydroxides, phosphides, selenides, nitrides, sulfides, borides, and carbides) have been developed as electrocatalysts for HER.[21–23] In general, there are three types of hybrid electrocatalysts with different interfaces: metal/metal, metal/compound, and compound/compound. Herein, we focus on interfacial electrocatalysts consisting of metal/compound interfaces. We particularly highlight their synthesis methods, reaction mechanisms, and electrocatalytic activities for HER. This article is structured primarily into two

Jian-Hong Tang, University of Cincinnati, USA; tangj4@ucmail.uc.edu
Yujie Sun, University of Cincinnati, USA; yujie.sun@uc.edu

doi:10.1557/mrs.2020.169

sections: noble metal- and non-noble metal-based hybrid electrocatalysts interfaced with various metal compounds.

Noble metal/compound-based hybrid electrocatalysts for H_2 evolution

Interfacing Pt with compounds

Pt is the state-of-the-art HER electrocatalyst in acidic electrolytes because of its good performance and properties. However, its catalytic activity is severely reduced under alkaline conditions due to sluggish water adsorption and dissociation steps.[16] It was recently found that interfacing Pt with transition-metal hydroxides was an effective strategy in boosting its HER performance in alkaline electrolytes. In 2011, Markovic et al. reported a new Pt electrode with electrochemically deposited $Ni(OH)_2$ nanoclusters that exhibited much enhanced HER activity relative to the parent Pt electrode at high pH.[16] In the hybrid $Ni(OH)_2$/Pt electrocatalyst, the $Ni(OH)_2$ nanoclusters act as the active sites for the adsorption and dissociation of water while Pt adsorbs the hydrogen intermediates for the eventual formation of H_2. A schematic cartoon of this is shown in **Figure 1**a. Such an interfacing strategy is effective for both Pt(111) and Pt(110) facets, In addition, the overall HER activity trend follows this order: Pt < $Ni(OH)_2$/Pt << $Ni(OH)_2$/Pt-islands (Pt surfaces modified by two-dimensional Pt/Pt) (Figure 1b). Furthermore, it was also revealed that solvated Li^+ ions could destabilize the H–OH bond of water and contribute to further enhancing the HER performance of $Ni(OH)_2$/Pt under alkaline conditions by at least two times. As shown in Figure 1c, the catalytic activity of the Pt(111) facet modified with various 3*d* transition-metal hydroxides follows the order of Ni > Co > Fe > Mn, which is inversely related to the binding strength of $OH–M^{2+\delta}$ (M: Ni < Co < Fe < Mn,: the changes in the valence states).[24]

The previously discussed works stimulated further investigations in hybrid Pt-based electrocatalysts interfaced with $Ni(OH)_2$ for improved HER performance. For instance, Tang et al. reported a new hybrid nanoarchitecture that was composed of one-dimensional ultrathin Pt nanowires (Pt NWs) interfaced with two-dimensional single-layered $Ni(OH)_2$ nanosheets (SL-$Ni(OH)_2$). The HER activity of this Pt NWs/SL-$Ni(OH)_2$ electrocatalyst was 4–5 times higher than that of commercial Pt/C.[25] Jin et al. reported a similar *in situ* reduction strategy to prepare Pt nanocrystals on single-layer $Ni(OH)_2$ nanosheets (Pt/2D-$Ni(OH)_2$). Pt/2D-$Ni(OH)_2$ showed a HER activity 5× higher than that of its commercial counterpart together with a decrease in overpotential by ~130 mV, contributing to a higher voltage efficiency, which was rationalized by the well-controlled growth of the Pt/$Ni(OH)_2$ interfaces.[26] Feliu and co-workers investigated the effect of different $Ni(OH)_2$ surface coverages on Pt(111) for improving the overall HER performance and proposed that changes in the reorganization energy of the interfacial water molecules play a critical role in affecting the H_2 evolution rate.[27]

In addition to Pt/$Ni(OH)_2$ interfaced electrocatalysts, the combination of other compounds with Pt has also been demonstrated to achieve enhanced performance of electrocatalytic H_2 evolution from water. For example, a Pt/Ni_3N electrocatalyst with a low Pt content of 15% was reported to achieve a current density of 200 mA cm^{-2} at an overpotential of 160 mV, a Tafel slope (describes the electrochemical kinetics relationship between the rate of an electrochemical reaction and the overpotential) of 36.5 mV dec^{-1}, an onset potential of 5 mV, and excellent stability for HER.[28] It was rationalized that the Ni_3N nanosheets possess high electron conductivity and their atomic thickness also creates abundant active sites for water adsorption and dissociation, all of which are beneficial for electrocatalytic H_2 generation. Sun and co-workers recently designed and studied Pt/$Ni(HCO_3)_2$ heterostructures for enhanced alkaline HER performance.[29] They found that $Ni(HCO_3)_2$ provides decent water adsorption/dissociation

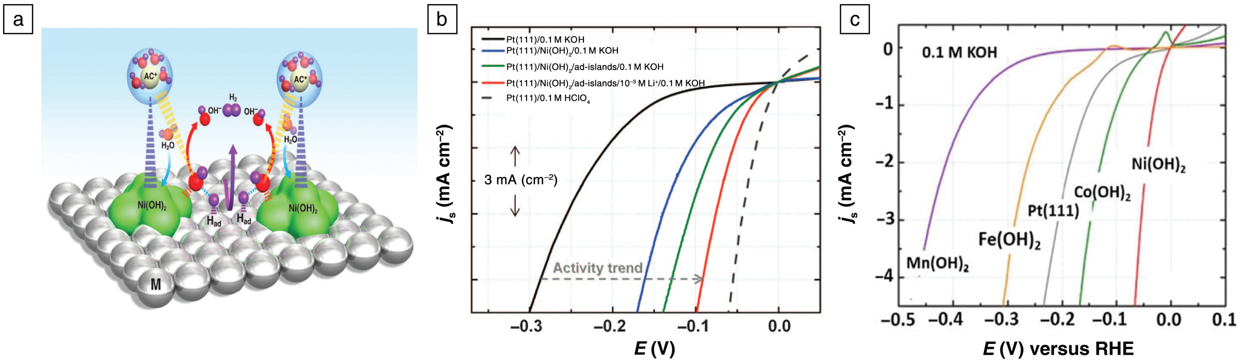

Figure 1. (a) Schematic representation of the H_2 evolution reaction (HER) mechanism at the $Ni(OH)_2$/Pt interface, including water dissociation, formation of M-H_{ad} intermediates, and recombination of two H_{ad} atoms to generate H_2.[19] (b) Comparison of the HER activities of Pt(111) with varying co-catalysts under different conditions. The increase in activity trend is shown by the dashed arrow.[19] (c) HER polarization curves for Pt(111) interfaced with various transition-metal hydroxides in 0.1 M KOH. Pt–$Ni(OH)_2$ is the most active catalyst and Pt–($Mn(OH)_2$) is the least active catalyst.[17] Note: Ac^+, cations; ad-islands, Pt surfaces modified by 2D Pt; M, Pt; j_s, current density; *E*, potential; RHE, reversible hydrogen electrode.

capability and intensive electronic interaction with Pt, both of which facilitate the HER activity in alkaline media.

Interfacing other noble metals with compounds

Despite the progress in developing Pt/compound-interfaced electrocatalysts for H_2 evolution, the scarcity and high cost of Pt inevitably limit its large-scale adoption. Therefore, considerable research efforts have been devoted to exploring alternative lower cost but with high performance HER electrocatalysts. For instance, a number of other noble metals (Au, Ru, Rh, and Pd) have been interfaced with various metal compounds to exhibit promising HER activity.

A photochemical reduction method was reported by Pande et al. to prepare Au/CuS heterostructures, which exhibited excellent HER performance under acidic conditions—the charge-transfer resistance from the catalyst to electrolyte decreased from 255.4 Ω for CuS to 31.1 Ω for Au/CuS.[30] More recently, Liu and co-workers reported a two-zone chemical vapor deposition method to fabricate Au/TaS_2, which exhibited a low overpotential requirement (101 mV at 10 mA cm^{-2}) and a small charge-transfer resistance (28 Ω at an overpotential of 80 mV) for HER. It was further discovered that the HER activity of these Au/TaS_2 electrocatalysts could be modulated via interfacial engineering, such as lattice mismatch and electron injection between TaS_2 and Au (**Figure 2**a).[31]

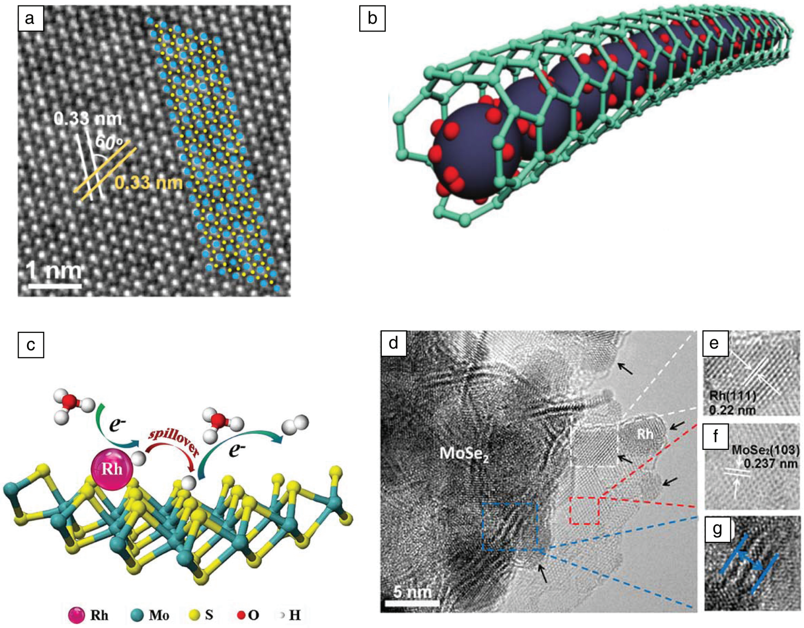

Figure 2. (a) High-resolution transmission electron microscope (TEM) image of Au/TaS_2. The blue spheres represent TaS_2, and the gold spheres represent Au.[31] (b) Schematic illustration of the Ru/WNO@C electrocatalyst. The violet core represents the WNO nanowire, the red pellets represent the Ru nanoclusters, the outer light blue shell represents the few-layer N-doped carbon.[32] (c) Scheme illustrating the H_2 evolution reaction mechanism on the Rh/MoS_2 catalyst. (Left to right) A hydrogen ion reacts with an electron to afford an H atom on the Rh surface; next, adsorbed neutral H atom transfers to the MoS_2 surface; finally, the H atom on the MoS_2 surface reacts with an electron and a hydrogen ion to form hydrogen.[33] (d) High-resolution TEM image of Rh/$MoSe_2$. The high magnification micrographs represent the HRTEM of (e, white) Rh, (f, red) one layer of $MoSe_2$ nanosheet, and (g, blue) three layers of $MoSe_2$ nanosheets.[34]

Li et al. synthesized cable-like Ru/WNO@C ($W_{0.62}(N_{0.62}O_{0.38})$ nanowires covered by few-layer N-doped carbon) with a Ru weight percentage of 3.37% by annealing $W_{18}O_{49}$ nanowires and $RuCl_3$ in molten urea. This Ru/WNO@C electrocatalyst (Figure 2b) showed a record-low overpotential of 2 mV to arrive at 10 mA cm^{-2} together with a Tafel slope of 33 mV dec^{-1} and long-term durability.[32] The superior HER activity of Ru/WNO@C was rationalized through density functional theory (DFT) calculations, which indicated a moderate hydrogen adsorption free energy (–0.21 eV) and a rather low water dissociation barrier (0.27 eV) on Ru/WNO@C.

Shao and co-workers developed a Rh-based hybrid electrocatalyst, 5.2 wt% Rh/MoS_2, which required a low overpotential of 47 mV to produce a current density of 10 mA cm^{-2}, as well as a small Tafel slope (24 mV dec^{-1}) and persistent stability. As shown in Figure 2c, the authors proposed a reaction mechanism involving three steps. First, a hydrogen ion reacts with an electron to afford an H atom on the Rh surface; secondly, the adsorbed neutral H atom transfers to the MoS_2 surface; and finally, the H atom on the MoS_2 surface reacts with an electron and a hydrogen ion to form hydrogen. It was concluded that the superior HER performance of Rh/MoS_2 resulted from the fast adsorption of hydronium ions on Rh followed by migration to the MoS_2 surface for H_2 evolution.[33] Recently, Chen et al. successfully fabricated an analogous Rh/$MoSe_2$ nanocomposite (TEM image shown in Figure 2d–g), which exhibited high HER activity with a low onset potential of 3 mV and a small overpotential of 31 mV to reach 10 mA/cm^2.[34]

Besides the previously mentioned noble metal/compound-interfaced electrocatalysts, Pd was also explored in hybrid HER electrocatalysts. For example, He et al. synthesized Pd/CeO_2/C via a two-step chemical deposition and reduction method, and the resulting Pd/CeO_2/C was observed to be a promising HER electrocatalyst in alkaline electrolytes. The formation of a Pd-O-Ce interfacial structure was confirmed by various characterization results, such as x-ray photoelectron spectroscopy and x-ray adsorption spectroscopy, and is believed to contribute to the overall HER activity.[35]

Non-noble metal-/compound-based hybrid electrocatalysts for H_2 evolution

It is exciting to see improved H_2 evolution rates on noble metal-/compound-interfaced electrocatalysts relative to pure noble metals, not only because of the enhanced electrocatalytic performance, but also because of the reduced amount of noble metals utilized in the hybrid electrocatalysts. Given the limited abundance and high cost of most noble metals, it would be more desirable to completely avoid the use of noble metals in electrocatalytic H_2 generation from water on a large scale. Consequently, the development of noble metal-free HER electrocatalysts with comparable or even higher activity has attracted increasing attention. The following highlights a few electrocatalytic systems consisting of only non-noble metals interfaced with diverse metal compounds. Such an interfacing strategy is equally effective in promoting the overall HER performance of many low-cost hybrid electrocatalysts.

Interfacing Ni with compounds

Benefiting from its excellent conductivity, chemical stability, and earth abundance, Ni has been a popular candidate for electrocatalytic H_2 generation under neutral and alkaline conditions. To date, a large number of metal compounds, ranging from oxides, hydroxides, phosphides, nitrides, to carbides, have been exploited to construct various Ni/compound-interfaced HER electrocatalysts.[36–45] In 2012, Danilovic et al. reported a Ni/Ni(OH)$_2$ electrocatalyst by decorating Ni(OH)$_2$ nanoclusters on a Ni electrode.[36] The HER activity of Ni/Ni(OH)$_2$ was enhanced by a factor of four compared to the pristine Ni electrode. Chhetri and co-workers recently fabricated a Ni/Ni(OH)$_2$/graphite electrode that achieved a HER current density of 200 mA/cm^2 at an overpotential of 0.3 V, superior to the activity of Pt (an overpotential of 0.44 V required to reach the same current density) under the same condition.[37]

Sun's group obtained a Ni/Ni$_2$P-interfaced electrocatalyst using a facile two-step method of template-free electrodeposition and low-temperature phosphidation.[42] As indicated by the scanning electron microscope (SEM) image in **Figure 3**a, Ni/Ni$_2$P on a Ni foam exhibited a three-dimensional (3D) hierarchically porous morphology with many stacked coarse particles (100–350 µm). Linear sweep voltammetry measurements (Figure 3b) revealed that this Ni/Ni$_2$P hybrid electrocatalyst achieved excellent HER activity, reaching 10 mA cm^{-2} at an overpotential of 98 mV and outperforming all the control samples without the Ni/Ni$_2$P interfaces. The combination of the electrochemically active constituents, 3D interconnected porosity, and high conductivity (Figure 3c) of Ni/Ni$_2$P all contribute to its outstanding HER performance. Zhang et al. subsequently unveiled an electrochemical-phosphorization method to construct Ni/NiP interfaces that achieved further improved HER activity, requiring an overpotential of only 69 mV to produce a current density of 10 mA cm^{-2}.[43] In addition to nickel phosphides, nickel nitrides have been utilized to interface with Ni for HER. For example, Sun et al. reported a Ni/Ni$_3$N electrocatalyst with extraordinary HER activity, exhibiting nearly zero onset overpotential and only 12–19 mV overpotential to produce 10 mA cm^{-2} (Figure 3d–e).[44] As shown in Figure 3d, high-resolution transmission electron microscopy of the Ni$_3$N/Ni interface showed both the (200) crystal plane of cubic Ni at an interplanar distance of 0.176 nm, and the (111) and (002) crystal planes of hexagonal Ni$_3$N at interplanar spacings of 0.204 and 0.214 nm, respectively, indicating the formation of the interface between cubic Ni and hexagonal Ni$_3$N. DFT calculations (Figure 3f) further corroborated the idea that the catalytic active sites of Ni/Ni$_3$N were located at the interface between Ni and Ni$_3$N.

Interfacing Co with compounds

Analogous to the Ni-based catalysts, Co has also been frequently explored as an electrocatalyst constituent for electrocatalytic water splitting to produce H_2. Interfacial Co/compound hybrids are another important class of noble metal-free electrocatalysts with intriguing HER activities.[46–50] In 2015, Chen and co-workers reported a 3D Co/Co$_3$O$_4$ electrocatalyst (**Figure 4**a) with a metallic Co core and an amorphous cobalt oxide shell structure. The synergistic effect of Co and Co$_3$O$_4$ provides both high conductivity and high surface activity, which are beneficial to high-performance HER activity, such as nearly zero onset potential and an overpotential of only 90 mV to reach 10 mA cm^{-2}.[49]

Similar to the preparation of Ni/Ni$_2$P previously mentioned, a one-step phosphorization was also adopted to transform a pre-oxidized Co foil to Co/Co$_2$P (Figure 4b). The obtained Co/Co$_2$P indeed exhibited better HER performance than the pristine Co foil, only requiring an overpotential of 157 mV to afford 10 mA cm^{-2}.[47] Besides phosphides, cobalt nitrides were also employed to be interfaced with Co for improved HER performance. Recently, Sun et al. reported an interfacial Co/Co$_2$N electrocatalyst that possessed HER activity superior to the state-of-the-art Pt counterpart tested under similar conditions (Figure 4c).[46] Co/Co$_2$N was able to produce a HER current density of 10 mA cm^{-2} at an overpotential of merely 12 mV in 1.0 M KOH, which was smaller than that required by Pt (20 mV). According to the DFT calculation results, the Co/Co$_2$N interfacial sites facilitated the adsorption and dissociation of water and optimized the free energy of hydrogen adsorption, both of which play critical roles in realizing its superior HER performance. It should be noted that Co/Co$_2$N is equally active for the opposite reaction of HER, electrocatalytic H_2 oxidation, which is another crucial reaction for the application of H_2 fuel cells. The dual functionality of Co/Co$_2$N further manifests the power of metal/compound interfacing engineering in the design and development of competent electrocatalysts for practical applications.

Interfacing other non-noble metals with compounds

In addition to the Ni/compounds and Co/compounds systems, other earth-abundant metals such as Cu, Fe, and Ti have also been applied in fabricating non-noble metals/compounds-interfaced HER electrocatalysts.[36,51–53] Zou et al. synthesized a Cu/CoS$_x$ electrocatalyst by directly depositing CoS$_x$ on a copper foam in ethanol at 70°C (Figure 4d).[51] The resulting Cu/CoS$_x$ material shows efficient HER activity with current densities of 10 and 100 mA cm^{-2} at overpotentials of 134 and

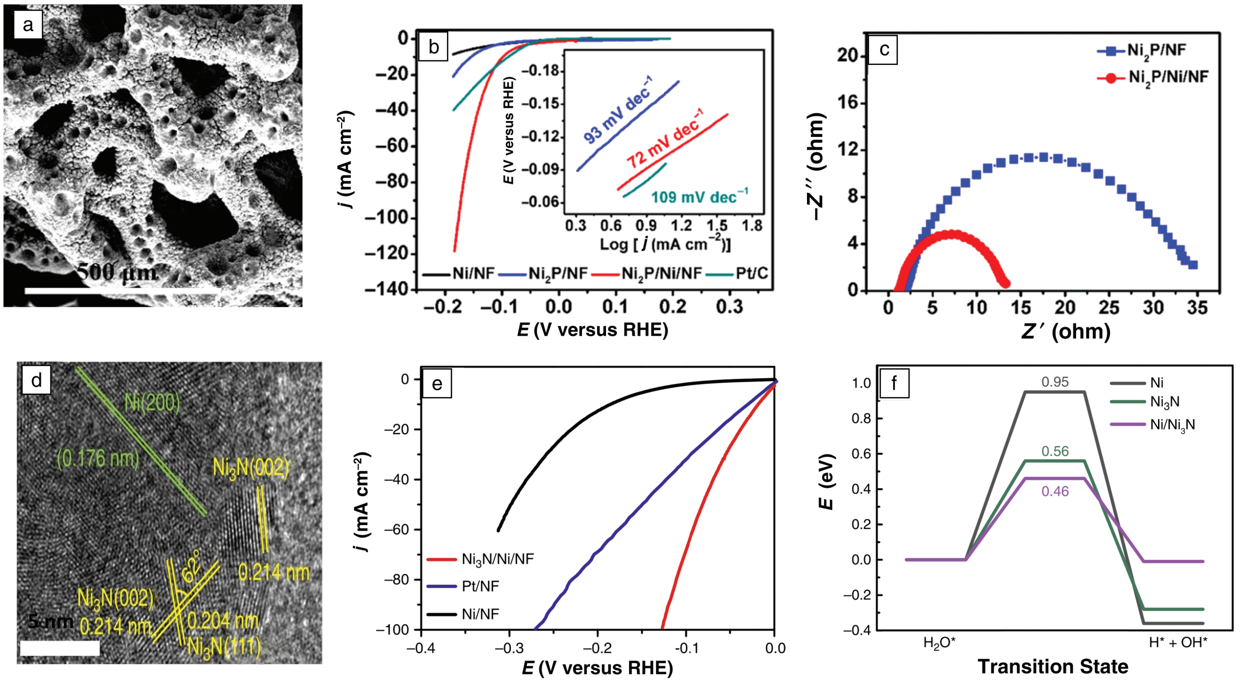

Figure 3. (a) Scanning electron microscope image of Ni/Ni$_2$P on nickel foam.[42] (b) H_2 evolution reaction (HER) polarization curves and (inset) the corresponding Tafel plots of Ni/Ni$_2$P and its control electrocatalysts. As compared to Pt/C, Ni$_2$P/Ni/NF shows the best H_2 evolution activity under identical conditions.[42] (c) Nyquist plots of Ni$_2$P/NF and Ni$_2$P/Ni/NF indicate that Ni$_2$P/Ni/NF exhibited a smaller semicircular diameter, suggesting a smaller contact and charge-transfer impedance.[42] (d) High-resolution transmission electron microscope image of Ni/Ni$_3$N showing the Ni/Ni$_3$N interface.[44] (e) HER polarization curves of Ni/NF, Ni$_3$N/Ni/NF, and Pt/NF electrocatalysts. Ni$_3$N/Ni/NF exhibits extraordinary HER activity and is superior to Pt/NF.[44] (f) Density functional theory calculated energy profiles for water dissociation on Ni, Ni$_3$N, and Ni/Ni$_3$N suggest that Ni/Ni$_3$N indicates the lowest energy barrier for water dissociation.[44] Note: *j*, current density; *E*, potential; RHE, reversible hydrogen electrode; NF, nickel foam; *Z*″, the imaginary part of an impedance; *Z*′, the real part of an impedance.

267 mV, respectively. Li and co-workers reported a hybrid electrocatalyst composed of Cu nanodots-decorated Ni$_3$S$_2$ nanotubes on carbon fibers (Cu/Ni$_3$S$_2$), which exhibited outstanding HER rates in alkaline media with a low onset overpotential of ~60 mV and overpotential of 128 mV at 10 mA cm^{-2} (Figure 4e).[52] It was reasoned that electronic interactions between Cu and Ni$_3$S$_2$ optimized hydrogen adsorption and desorption on the catalyst surface and improved the electrocatalytic activity. It required an overpotential of 128 mV at 10 mA cm^{-2} together with excellent durability. Hu et al. developed a Fe/Fe$_x$S$_y$ electrocatalyst via a facile one-step electrodeposition method (Figure 4f). Compared to the Fe counterpart, Fe/Fe$_x$S$_y$ exhibited a much enhanced HER activity benefiting from the synergistic effects of interfacing Fe with Fe$_x$S$_y$.[53]

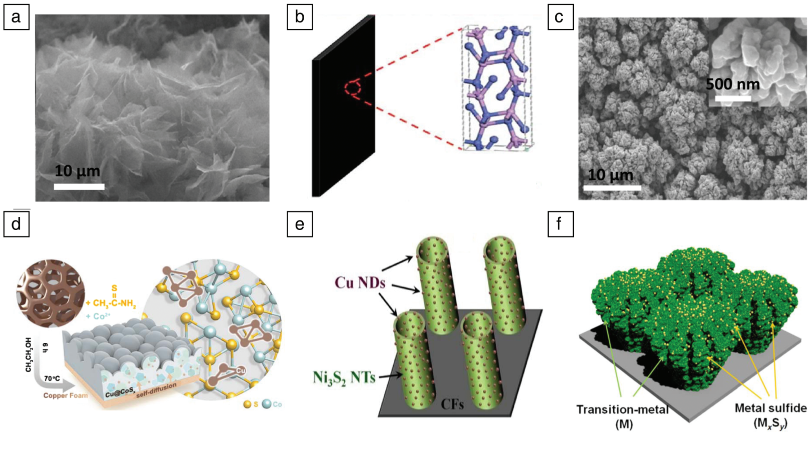

Figure 4. (a) Scanning electron microscope (SEM) image of Co/Co$_3$O$_4$ nanosheet.[49] (b) Schematic illustration of the Co/Co$_2$P electrode. The (left) Co-foil and (right) Co$_2$P. Blue indicates P and purple represents Co.[47] (c) SEM image of Co/Co$_2$N on a cobalt foam. The inset shows the image at a 500-nm scale.[46] (d) Schematic illustration of the synthesis of Cu/CoS$_x$ electrocatalyst via a low-temperature synthetic route involving the interdiffusion of copper species from copper foam into the CoS$_x$ film.[51] Cartoon representations of (e) Cu/Ni$_3$S$_2$ on carbon fibers (CFs)[52] and (f) Fe/Fe$_x$S$_y$ electrocatalyst.[53] Note: NTs, nanotubes; NDs, nanodots; M, Fe.

Summary and outlook

In this article, we have summarized recent advances in HER electrocatalysis employing metal/compound-interfaced systems as electrocatalysts. It is apparent that by interfacing metals with appropriate metal compounds, whether using noble metals or non-noble metals, greatly improved HER performance was achieved relative to their pure metal counterparts. Such an interfacing engineering strategy not only lowers the required amount of metal, particularly attractive for noble metal-containing electrocatalysts, but also creates unique and novel active sites located at the metal/compound interfaces. In the meantime, the metal components can still provide excellent conductivity for effective electron transfer between the electrode and electrolyte.

Even though Pt-based electrocatalysts remain state-of-the-art HER electrocatalysts, the rapid development of lower-cost alternative candidates has substantially narrowed their activity gap from noble metal-based catalysts. For instance, several Ni-based electrocatalysts, such as Ni/Ni_3N, exhibit outstanding HER activity in alkaline media, which is comparable to or even superior to that of commercially available Pt/C. In addition to the exciting findings regarding interfacing metals and compounds for electrocatalytic H_2 production from water, it is anticipated that more creative hybrid electrocatalysts taking advantage of the interfacing engineering strategy will appear continuously.

Nevertheless, in order to expedite the advancement of interfacial HER electrocatalysts, it is of critical importance to understand the intrinsic activities of the interfacial sites between metals and compounds. Currently, DFT calculations have been frequently employed to elucidate the beneficial impact of interfacing metals with compounds and strongly imply that the real active sites are indeed located as the interfaces. Nevertheless, more definitive experimental evidence is still needed for most systems. Therefore, *in situ* electrocatalytic characterization coupled with spectroscopic investigations are highly desired to provide more detailed information regarding the function of interfacial sites. In order to gain these experimental results, model catalysts with well-defined interfacial sites should be synthesized first, which await further experimental efforts.

Acknowledgments

Y.S. acknowledges the financial support of the Herman Frasch Foundation (820-HF17), the National Science Foundation (CHE1914546), and the University of Cincinnati.

References

1. M. Dresselhaus, I. Thomas, *Nature* **414**, 332 (2001).
2. S. Chu, A. Majumdar, *Nature* **488**, 294 (2012).
3. N. Linares, A.M. Silvestre-Albero, E. Serrano, J. Silvestre-Albero, J. Garcia-Martinez, *Chem. Soc. Rev.* **43**, 7681 (2014).
4. C. Tang, H.F. Wang, Q. Zhang, *Acc. Chem. Res.* **51**, 881 (2018).
5. Z. Yang, J. Zhang, M.C. Kintner-Meyer, X. Lu, D. Choi, J.P. Lemmon, J. Liu, *Chem. Rev.* **111**, 3577 (2011).
6. J.A. Turner, *Science* **285**, 687 (1999).
7. L. Han, S.J. Dong, E.K. Wang, *Adv. Mater.* **28**, 9266 (2016).
8. J. Wang, F. Xu, H.Y. Jin, Y.Q. Chen, Y. Wang, *Adv. Mater.* **29**, 1605838 (2017).
9. X.X. Zou, Y. Zhang, *Chem. Soc. Rev.* **44**, 5148 (2015).
10. Y. Jiao, Y. Zheng, M.T. Jaroniec, S.Z. Qiao, *Chem. Soc. Rev.* **44**, 2060 (2015).
11. J.H. Wang, W. Cui, Q. Liu, Z.C. Xing, A.M. Asiri, X.P. Sun, *Adv. Mater.* **28**, 215 (2016).
12. Y.M. Shi, B. Zhang, *Chem. Soc. Rev.* **45**, 1529 (2016).
13. I. Roger, M.A. Shipman, M.D. Symes, *Nat. Rev. Chem.* **1**, 0003 (2017).
14. S. Anantharaj, S.R. Ede, K. Sakthikumar, K. Karthick, S. Mishra, S. Kundu, *ACS Catal.* **6**, 8069 (2016).
15. Y. Zheng, Y. Jiao, A. Vasileff, S.Z. Qiao, *Angew. Chem. Int. Ed. Engl.* **57**, 7568 (2018).
16. R. Subbaraman, D. Tripkovic, D. Strmcnik, K.-C. Chang, M. Uchimura, A.P. Paulikas, V. Stamenkovic, N.M. Markovic, *Science* **334**, 1256 (2011).
17. D. Strmcnik, P.P. Lopes, B. Genorio, V.R. Stamenkovic, N.M. Markovic, *Nano Energy* **29**, 29 (2016).
18. Q. Shao, P.T. Wang, X.Q. Huang, *Adv. Funct. Mater.* **29**, 1806419 (2019).
19. N. Dubouis, A. Grimaud, *Chem. Sci.* **10**, 9165 (2019).
20. B. Ruqia, S.I. Choi, *ChemSusChem* **11**, 2643 (2018).
21. J. Zhang, Q. Zhang, X. Feng, *Adv. Mater.* **1808167** (2019).
22. H. Li, C. Chen, D. Yan, Y. Wang, R. Chen, Y. Zou, S. Wang, *J. Mater. Chem.* A **7**, 23432 (2019).
23. T. Kwon, M. Jun, J. Joo, K. Lee, *J. Mater. Chem.* A **7**, 5090 (2019).
24. R. Subbaraman, D. Tripkovic, K.-C. Chang, D. Strmcnik, A.P. Paulikas, P. Hirunsit, M. Chan, J. Greeley, V. Stamenkovic, N.M. Markovic, *Nat. Mater.* **11**, 550 (2012).
25. H. Yin, S. Zhao, K. Zhao, A. Muqsit, H. Tang, L. Chang, H. Zhao, Y. Gao, Z. Tang, *Nat. Commun.* **6**, 6430 (2015).
26. L. Wang, Y. Zhu, Z. Zeng, C. Lin, M. Giroux, L. Jiang, Y. Han, J. Greeley, C. Wang, J. Jin, *Nano Energy* **31**, 456 (2017).
27. F.J. Sarabia, P. Sebastián-Pascual, M.T. Koper, V. Climent, J.M. Feliu, *ACS Appl. Mater. Interfaces* **11**, 613 (2018).
28. Y. Wang, L. Chen, X. Yu, Y. Wang, G. Zheng, *Adv. Energy Mater.* **7**, 1601390 (2017).
29. M. Lao, K. Rui, G. Zhao, P. Cui, X. Zheng, S.X. Dou, W. Sun, *Angew. Chem. Int. Ed. Engl.* **58**, 5432 (2019).
30. M. Basu, R. Nazir, P. Fageria, S. Pande, *Sci. Rep.* **6**, 34738 (2016).
31. Q. Yu, Y. Luo, S. Qiu, Q. Li, Z. Cai, Z. Zhang, J. Liu, C. Sun, B. Liu, *ACS Nano* **13**, 11874 (2019).
32. L.-N. Zhang, Z.-L. Lang, Y.-H. Wang, H.-Q. Tan, H.-Y. Zang, Z.-H. Kang, Y.-G. Li, *Energy Environ. Sci.* **12**, 2569 (2019).
33. Y. Cheng, S. Lu, F. Liao, L. Liu, Y. Li, M. Shao, *Adv. Funct. Mater.* **27**, 1700359 (2017).
34. S. Liu, M. Li, C. Wang, P. Jiang, L. Hu, Q. Chen, *ACS Sustain. Chem. Eng.* **6**, 9137 (2018).
35. T. Gao, J. Yang, M. Nishijima, H.A. Miller, F. Vizza, H. Gu, H. Chen, Y. Hu, Z. Jiang, L. Wang, *J. Electrochem. Soc.* **165**, F1147 (2018).
36. N. Danilovic, R. Subbaraman, D. Strmcnik, K.C. Chang, A. Paulikas, V. Stamenkovic, N.M. Markovic, *Angew. Chem. Int. Ed. Engl.* **51**, 12495 (2012).
37. M. Chhetri, S. Sultan, C. Rao, *Proc. Natl. Acad. Sci. U.S.A.* **114**, 8986 (2017).
38. Z. Weng, W. Liu, L.-C. Yin, R. Fang, M. Li, E.I. Altman, Q. Fan, F. Li, H.-M. Cheng, H. Wang, *Nano Lett.* **15**, 7704 (2015).
39. M. Gong, W. Zhou, M.-C. Tsai, J. Zhou, M. Guan, M.-C. Lin, B. Zhang, Y. Hu, D.-Y. Wang, J. Yang, *Nat. Commun.* **5**, 4695 (2014).
40. X. Liu, K. Ni, C. Niu, R. Guo, W. Xi, Z. Wang, J. Meng, J. Li, Y. Zhu, P. Wu, *ACS Catal.* **9**, 2275 (2019).
41. D. Ji, L. Peng, J. Shen, M. Deng, Z. Mao, L. Tan, M. Wang, R. Xiang, J. Wang, S.S.A. Shah, *Chem. Commun.* **55**, 3290 (2019).
42. B. You, N. Jiang, M. Sheng, M.W. Bhushan, Y. Sun, *ACS Catal.* **6**, 714 (2016).
43. K. Xiong, Y. Gao, J. Chen, Y. Shen, H. Zhang, *Chem. Commun.* **56**, 611 (2019).
44. F. Song, W. Li, J. Yang, G. Han, P. Liao, Y. Sun, *Nat. Commun.* **9**, 4531 (2018).
45. Y.-Y. Ma, Z.-L. Lang, L.-K. Yan, Y.-H. Wang, H.-Q. Tan, K. Feng, Y.-J. Xia, J. Zhong, Y. Liu, Z.-H. Kang, *Energy Environ. Sci.* **11**, 2114 (2018).
46. F. Song, W. Li, J. Yang, G. Han, T. Yan, X. Liu, Y. Rao, P. Liao, Z. Cao, Y. Sun, *ACS Energy Lett.* **4**, 1594 (2019).
47. C.-Z. Yuan, S.-L. Zhong, Y.-F. Jiang, Z.K. Yang, Z.-W. Zhao, S.-J. Zhao, N. Jiang, A.-W. Xu, *J. Mater. Chem. A* **5**, 10561 (2017).
48. H. Wang, S. Min, Q. Wang, D. Li, G. Casillas, C. Ma, Y. Li, Z. Liu, L.-J. Li, J. Yuan, *ACS Nano* **11**, 4358 (2017).
49. X. Yan, L. Tian, M. He, X. Chen, *Nano Lett.* **15**, 6015 (2015).
50. C. Zhu, A.L. Wang, W. Xiao, D. Chao, X. Zhang, N.H. Tiep, S. Chen, J. Kang, X. Wang, J. Ding, *Adv. Mater.* **30**, 1705516 (2018).
51. Y. Liu, Q. Li, R. Si, G.D. Li, W. Li, D.P. Liu, D. Wang, L. Sun, Y. Zhang, X. Zou, *Adv. Mater.* **29**, 1606200 (2017).
52. J.-X. Feng, J.-Q. Wu, Y.-X. Tong, G.-R. Li, *J. Am. Chem. Soc.* **140**, 610 (2018).
53. Y. Sun, C. Huang, J. Shen, Y. Zhong, J. Ning, Y. Hu, *J. Colloid Interface Sci.* **558**, 1 (2019).

Jian-Hong Tang is a postdoctoral researcher at the University of Cincinnati. He received his PhD degree in 2018 from the Institute of Chemistry, Chinese Academy of Sciences, China. His research interests include ruthenium (II) complexes for photocatalysis, luminescence sensing, and phototherapy. Tang can be reached by email at tangj4@ucmail.uc.edu.

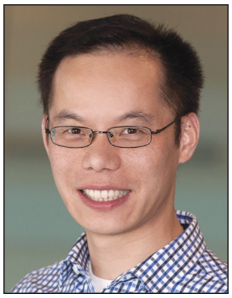

Yujie Sun has been an associate professor at the University of Cincinnati since 2018. Previously, he was an assistant professor at Utah State University. He received his BS degree in chemistry from Fudan University, China, in 2005, and his PhD degree from The Ohio State University in 2010. He completed postdoctoral research at the University of California, Berkeley, and the Lawrence Berkeley National Laboratory. His current research focuses on developing and understanding inexpensive materials and complexes for energy catalysis and biomedical applications. Sun can be reached by email at yujie.sun@uc.edu.